UiO : Department of Mathematics
University of Oslo

# Monolithic solver for Computational Fluid Structure Interaction

**Sebastian Gjertsen**

Master's Thesis, Spring 2017

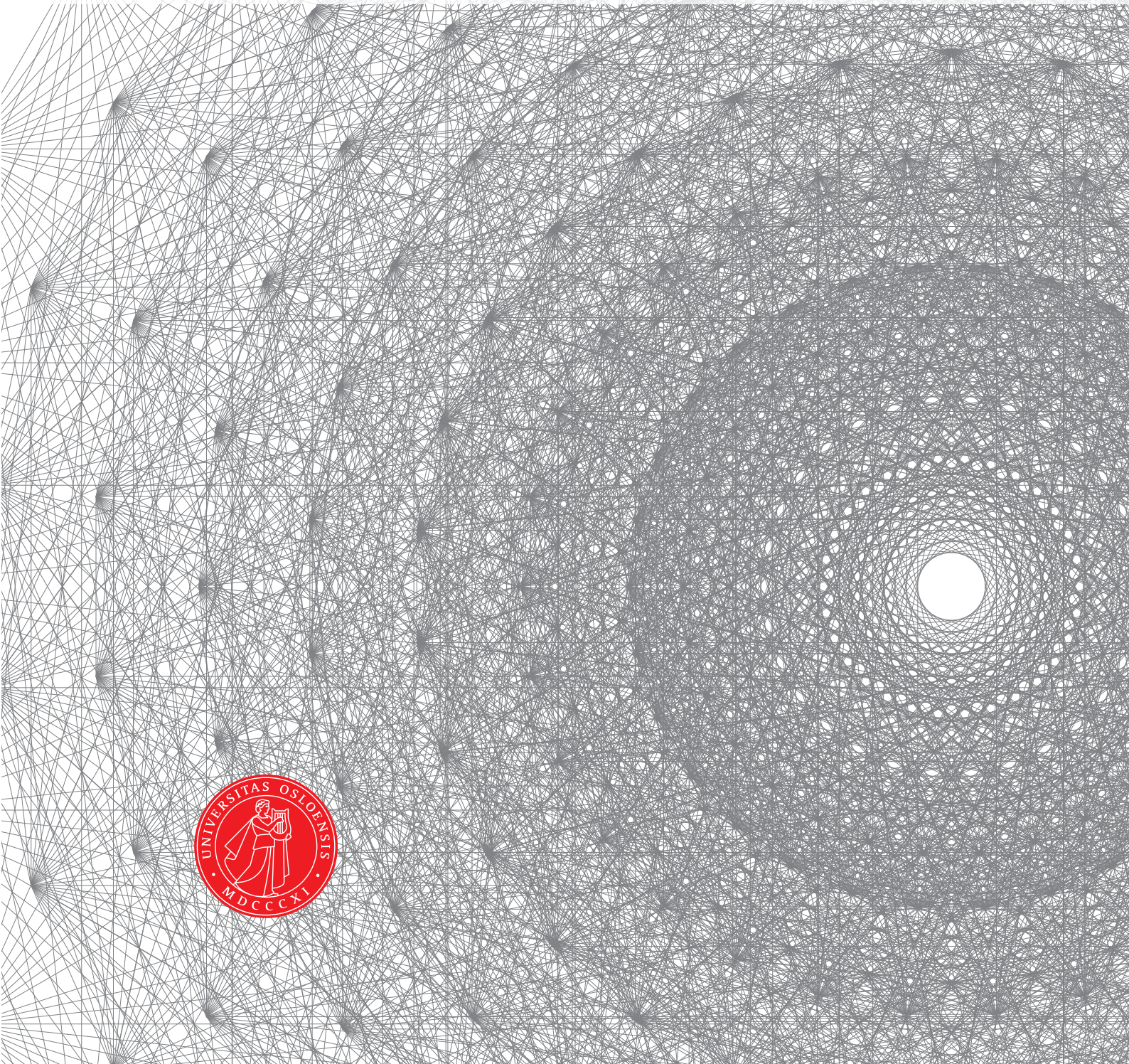

This master's thesis is submitted under the master's programme *Computational Science and Engineering*, with programme option *Mechanics*, at the Department of Mathematics, University of Oslo. The scope of the thesis is 60 credits.

The front page depicts a section of the root system of the exceptional Lie group $E_8$, projected into the plane. Lie groups were invented by the Norwegian mathematician Sophus Lie (1842–1899) to express symmetries in differential equations and today they play a central role in various parts of mathematics.

# Contents

# Chapter 1

# Introduction to Fluid-Structure Interaction

The interaction between fluids and structures can be observed all around us in nature. From a flag waving in the wind to a large windmill at sea, when we breath in air and our lungs expand, when our hearts fill up with blood and muscles contract to push blood into our arteries, are all examples of fluids and structures interacting. A flag waving in the wind is mainly air(fluid) exerting force on the flag(structure), making the flag flutter. However, the structure can also move the fluid. When we breathe air into our lungs, our diaphram contracts and moves downward, increasing the space in our chest cavity making the lungs expand. As the lungs expand air is sucked through the mouth and nose, filling up the lungs. In this manner both fluid and structures can exert force, and consequently interact with each other.

A bridge is an example of Fluid-Structure Interaction(FSI), where the bridge is a rigid structure, with wind interacting with the structure. A profound example of wind interacting with a bridge, is the collapse of the Tacoma Narrows Bridge in 1940 [1]. The bridge collapsed only two months after being opened. The collapse was due to strong winds(64 km/h) interacting with the bridge, making the bridge flutter and ultimately collapse. No human life was lost in the collapse, but a Cocker Spaniel named Tubby left in a car was not so lucky.

Modeling FSI is used today when constructing for instance windmills. Windmills are usually rigid, hence giving a big difference in density between fluid and structure. The structure will in the case of a windmill only give rise

Figure 1.1: Tacoma bridge still standing with large deformations

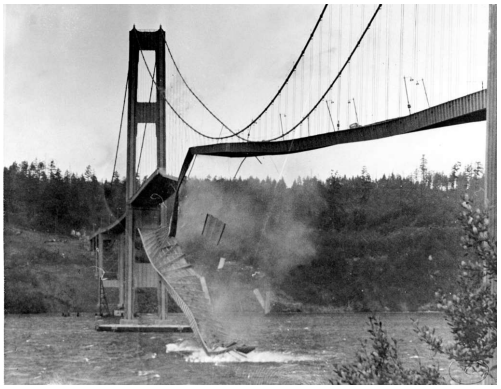

Figure 1.2: Tacoma bridge collapsed

to small deformations. However, modeling FSI in hemodynamics(dynamics of blood flow) deems more challenging. In the latter cases the densities in fluid and structure are more similar and blood flow usually induces large deformations in the veins and arteries. In both cases the fluid flow tends to transitions towards turbulence. All of these cases have challenges which gives the need to have rigid stabile FSI solvers. Solvers which can handle large deformations and high fluid velocity.

A branch of fluid dynamics is called Computational Fluid Dynamics, where computers and numerical analysis is used to solve fluid problems. I would argue that a similar name is used for FSI, namely *Computational Fluid Structure Interaction* (CFSI). However in the literature FSI is used to describe CFSI and the name FSI will be used in this thesis. Also, even though FSI is Fluid-*Structure* Interaction, the word solid will also be used to describe a structure.

The main goal of this master thesis is to build a framework to solve FSI problems, investigating different approaches and schemes. The framework will be validated and verified using the *Method of Manufactured Solutions*, accompanying a classic, well known benchmark, known to test the robustness of a FSI solver.

# Chapter 2

# Continuum mechanics in different frames of reference

All materials are made up of atoms. Between atom there is vacuum. The laws that govern atoms, are complex and very difficult to model. The length scales at which atoms are defined is in the nanometer ($10^{-9}m$) range. However, if we zoom out to the *macroscale*, the scale on which phenomena are large enough to be visible for the human eye, matter like solids and fluids can be modeled if we assume them to exist as a continuum. The continuum hypothesis states that there exist no space inside the matter and the matter completely fills up the space it occupies. We can use mathematics with basic newtonian physical laws to model fluids and solids when they are assumed continuous. These newtonian laws are generally expressed in two frames of reference, Lagrangian and Eulerian, depending on the the scientific branch.

To exemplify these frameworks we can imagine a river running down a mountain. In the Eulerian framework we are the observer standing besides the river looking at the flow. We are not interested in each fluid particle but only how the fluid acts as a whole flowing down the river. The Eulerian approach fits the fluid problem as we can imagine the fluid continuously deforming along the river side.

In the Lagrangian description we have to imagine ourselves on a leaf going down the river with the flow. Looking out as the mountain moves and we stand still compared to the fluid particles. The Lagrangian description fits a solid problem since we are generally interested in where the solid particles are

in relation to each other. For instance modeling a deflecting beam attached to a wall. To model this deflection one needs to know where all the particles are compared to each other. The more force that is applied the more the particles move in relation to each other. The Lagrangian description helps us to easier model a problem where need to know the particles spatial-relation to each other

This chapter introduces briefly the fluid and solid equations with their respective boundary conditions. A detailed description of the Lagrangian framework and the stress and strain relations are covered in the appendix.

## 2.1 Solid equation

The solid equation describes the motion of a solid. It is derived from the principles of conservation of mass and momentum. The solid equation is stated in the Lagrangian reference system [8], in the solid time domain $\mathcal{S}$ as:

$$\rho_s \frac{\partial \mathbf{d}^2}{\partial t^2} = \nabla \cdot (P) + \rho_s f \quad in \ \mathcal{S} \tag{2.1}$$

written in terms of the deformation $\mathbf{d}$. P is the first Piola-Kirchhoff stress tensor. See Appendix for a detailed description of strain and stress leading to the Piola-Kirchhoff stress tensor. $f$ is a force acting on the solid body.

## 2.2 Fluid equations

The fluid equations are stated in an Eulerian framework. In the Eulerian framework the domain has fixed spatial points where the fluid passes through. The Navier-Stokes(N-S) equations are, like the solid equation, derived using principles of mass and momentum conservation. N-S describes the velocity and pressure in a given fluid continuum. Written in the fluid time domain $\mathcal{F}$ as an incompressible fluid:

$$\rho_f\big(\frac{\partial \mathbf{u}}{\partial t} + \mathbf{u} \cdot \nabla \mathbf{u}\big) = \nabla \cdot \sigma_f + \rho_f f \quad in \ \mathcal{F} \tag{2.2}$$

$$\nabla \cdot \mathbf{u} = 0 \quad in \ \mathcal{F} \tag{2.3}$$

where $\mathbf{u}$ is the fluid velocity, $p$ is the fluid pressure, $\rho$ stands for density. f is body force and $\sigma_f$ is the Cauchy stress tensor, $\sigma_f = \mu_f(\nabla \mathbf{u} + \nabla \mathbf{u}^T) - pI$

denoting a newtonian fluid. $I$ is the Identity matrix.

There does not yet exist an analytical solutions to the N-S equations for every fluid problem. Only simplified fluid problems can be solved [13] analytically using the N-S equations. Actually there is a prize set out by the Clay Mathematics Institute of 1 million dollars to whomever can show the existence and smoothness of Navier-Stokes solutions [3], as apart of their millennium problems. Nonetheless this does not stop us from discretizing and solving N-S numerically.

One difficulty in the N-S equations is the nonlinearity appearing in the convection term on the left hand side. Non-linearity is most often handled using a lagging velocity function, Newtons method, or Picard iterations. Another difficulty is finding a suitable equation to solve for the pressure field [2]. The difficulty with pressure has been tackled using for instance the incremental pressure correction scheme (IPCS).

## 2.3 Fluid and Structure Boundary conditions

To complete the fluid and solid equations, boundary conditions need to be imposed. The fluid flows and the solid moves within the boundaries noted as $\partial\mathcal{F}$ and $\partial\mathcal{S}$ respectively.

On the Dirichlet boundary, $\partial\mathcal{F}_D$ and $\partial\mathcal{S}_D$, we impose a given value. Dirichlet conditions can be initial conditions or set values, such as zero on the fluid boundary for a "no slip" condition. The Dirichlet conditions are defined for $\mathbf{u}$ and $p$ :

$$\mathbf{u} = u_0 \text{ on } \partial\mathcal{F}_D \tag{2.4}$$

$$p = p_0 \text{ on } \partial\mathcal{F}_D \tag{2.5}$$

$$\mathbf{d} = d_0 \text{ on } \partial\mathcal{S}_D \tag{2.6}$$

$$\mathbf{w}(\mathbf{X}, t)_0 = \frac{\partial \mathbf{d}(t=0)}{\partial t} \text{ on } \partial\mathcal{S}_D \tag{2.7}$$

The forces on the boundaries equal an eventual external force $\mathbf{f}$. These are are enforced on the Neumann boundaries $\partial\mathcal{F}_N$ and $\partial\mathcal{S}_N$ :

$$\sigma \cdot \mathbf{n} = f \text{ on } \partial\mathcal{F}_N \tag{2.8}$$

$$P \cdot \mathbf{n} = f \text{ on } \partial\mathcal{S}_N \tag{2.9}$$

# Chapter 3

# Fluid Structure Interaction Problem

The following chapter will be devoted to introducing the full FSI problem, with all the equations, conditions, and discretizations needed to to build a Fluid Structure Interaction solver.

When computing FSI problems the computing domain is split into three parts, fluid, structure, and interface. Fluid and structure domains are separated, and different constitutive equations are solved in each domain. The spatial points in which fluid and structure join is called the interface. The treatment of the interface gives the two main methods for solving FSI problems [6]. The first method is called fully Eulerian. In a fully Eulerian framework, both the fluid and structure equations are defined and solved in a purely Eulerian description. The interface in a fully Eulerian framework is tracked across a fixed domain [11]. The fully Eulerian description is suited for fluid problems but is problematic for structure problem. And certainly for FSI problems where tracking of the interface across the domain is a difficult task.

The second approach is the *Arbitrary Lagrangian Eulerian*(ALE). The ALE method entails formulating the fluid equations in a type of Eulerian framework and the solid in a Lagrangian framework. The entire domain itself moves with the structural displacements and the fluid moves through these points. In the ALE framework we get the best of both worlds, in that fluid and solid are described in their natural states. The structure equation will

remain as previously stated (2.1), and we will need to change the fluid equations to take into account the moving domain changing the fluid velocity.

Dealing with the movement of the domain is done in two ways. One way is to move the domain itself in relation to the structural displacements, and use this new domain to calculate the equations for every iteration. Moving the domain gives advantages as we can explicitly represent the fluid-structure interface, and the equations are stated in a more familiar manner. But problems arise when there are large deformations in the solid giving large deformations into the fluid domain. Moving the mesh with large deformation can be a challenge in that the domain can overlap causing singularities.

The second approach to ALE, which will be used in this thesis, is to calculate from **reference frame**. When solving equations from a reference frame we solve the equations on an initial, stress free domain, and use a series of mappings to account for the movements of the current time domain. It is the displacements in the in the domain that determines the value of the mappings between frames of reference.

From a technical point of view, moving both the mesh and using a reference frame are equivalent [8]. Since the reference frame method does not need a function to move the mesh between each time iteration, it can be less time consuming. The interface is also located in the same position, making the interface easy to track.

There are generally two types approaches when discretizing an FSI scheme. The first is the partitioned approach where fluid and structure are solved sequentially. The partitioned approach is appealing in that we have a wealth of knowledge and techniques on how to solve each of these kinds of problems in an efficient manner. The difficulty however is dealing with the interface. There are kinematic and dynamic conditions needed in FSI, and the coupling of these conditions is where problems arise. Explicit coupling schemes are known to be unconditionally unstable for standard Dirichlet-Neumann strategies when there is a large amount of added-mass in the system [5, 12]. There are however, schemes which offer added-mass free stability with explicit coupling, where the interface is treated through a Robin-Neumann coupling. The first scheme was made for coupling of a thin walled structure by Fernandez et al., 2013 [4]. Later a scheme was made with an extension coupling with a thick walled structure by Fernandez et.al,2015 [5]. The scheme for coupling

thick walled structures is rather complex and uses a number of techniques that are out of the scope of this thesis. ( This may be in more detail in a later chapter (discussion and further work.) )

In this thesis the other approach is used, named monolithic. In the monolithic approach all of the equations are solved at once. The monolithic approach has the advantage of offering numerical stability for problems with strong added-mass effects [6], and are fully coupled. The disadvantage over the partitioned approach is that we loose flexibility when solving many equations simultaneously, and the computing matrices can quickly become large and computationally costly. But the overall the ease of implementation and numerical stability makes monolithic the preferred choice in this thesis.

The following chapter starts by introducing the mappings needed to change between current and reference domain. Lastly, the equations will be discretized following the notation and ideas from [8]:

## 3.1 Mapping between different frames of reference

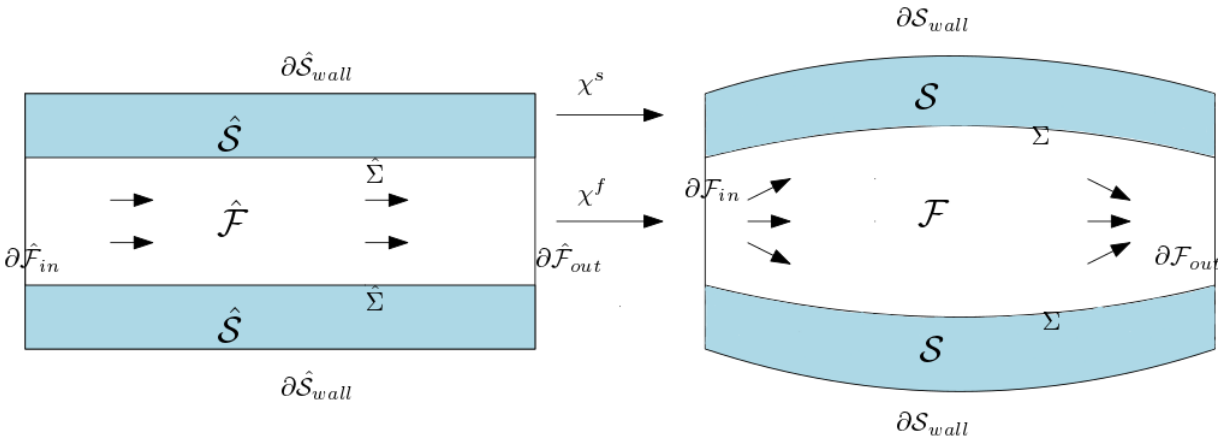


Figure 3.1: Mapping of domain from reference to current

Let $\hat{\mathcal{V}}$ be a reference volume and $\mathcal{V}(t)$ be the current time volume. Then using (A.5) and (A.6) to define a mapping between the volumes from the current to the reference configurations:

$$\int_{\mathcal{V}(t)} 1dx = \int_{\hat{\mathcal{V}}} Jdx \tag{3.1}$$

The gradients acting on a vector $\mathbf{u}$ will also be mapped between current and reference configurations:

$$\int_{\mathcal{V}(t)} \nabla \mathbf{u} dx = \int_{\hat{\mathcal{V}}} J \nabla \mathbf{u} F^{-1} dx \tag{3.2}$$

The divergence of a vector $\mathbf{u}$ will be mapped between configurations as:

$$\int_{\mathcal{V}(t)} \nabla \cdot \mathbf{u} dx = \int_{\hat{\mathcal{V}}} \nabla \cdot (J F^{-1} \mathbf{u}) dx \tag{3.3}$$

## 3.2 Governing equations for Fluid Structure Interaction

The following section formulates the equations in the Eulerian, Lagrangian, and the ALE description. I start by Briefly talking about time derivatives in the different configurations, to understand the need to change the fluid equation in the ALE description [14]:

### 3.2.1 Derivatives in different frameworks

In the Lagrangian framework the total and partial derivatives have the following relation:

$$D_t f(x,t) = \partial_t f(x,t) \tag{3.4}$$

The total and partial derivatives have the following relation in the Eulerian framework:

$$D_t f(x,t) = \mathbf{u} \cdot \nabla f + \partial_t f(x,t) \tag{3.5}$$

whilst in the ALE framework this concept is extended to take into account the motion of the domain:

$$D_t f(x,t) = \mathbf{w} \cdot \nabla f + \partial_t f(x,t) \tag{3.6}$$

Equation 3.6 shows that in the Lagrangian framework $\mathbf{w}$ is zero and for the Eulerian framework $\mathbf{w} = \mathbf{u}$.

### 3.2.2 Solid equation

Let $\Omega \in \hat{\mathcal{S}} \cup \hat{\mathcal{F}}$ be a global domain that is made up of the fluid, structure, and the interface. The interface is stated as: $\hat{\Sigma} \in \hat{\mathcal{S}} \cap \hat{\mathcal{F}}$. Let $\mathbf{u}$ be a global velocity function that describes the fluid velocity in the fluid domain and the structure velocity in the structure domain, $\mathbf{u} = \mathbf{u_s} \cup \mathbf{u_f} \in \Omega$. The deformation function is also defined as a global function $\mathbf{d} = \mathbf{d_s} \cup \mathbf{d_f} \in \Omega$. Using global velocity and displacement functions makes the velocity and displacement continuous across the entire domain. This is a nice feature which will be apparent once the interface conditions are stated. .

The solid equation will be written in terms of the solid velocity $\mathbf{u_s}$, in contrast to 2.1 which was written in terms of the deformation. Expressing the solid balance laws in the Lagrangian formulation from the initial configuration:

$$\rho_s \frac{\partial \mathbf{u}}{\partial t} = \nabla \cdot (P) + \rho_s f \quad in \quad \hat{\mathcal{S}} \tag{3.7}$$

### 3.2.3 Fluid equations

In the ALE description the fluid domain is moving, giving the need to redefine the velocity in the convective term in (2.2) to account for the moving domain:

$$\mathbf{u} \cdot \nabla \mathbf{u} \rightarrow (\mathbf{u} - \frac{\partial \mathbf{d}}{\partial t}) \cdot \nabla \mathbf{u} \tag{3.8}$$

Where $\mathbf{d}$ is the deformation in the fluid domain. The domain velocity $\mathbf{w} = \frac{\partial \mathbf{d}}{\partial t}$ is written in terms of the deformation as the partial time derivative.

The change in the fluid equations denoted from the current configuration using the aforementioned mappings, maps the fluid equations to the reference configuration:

$$\int_{\mathcal{V}(t)} \rho_f \frac{\partial \mathbf{u}}{\partial t} = \int_{\hat{\mathcal{V}}} \rho_f J \frac{\partial \mathbf{u}}{\partial t} dx \tag{3.9}$$

$$\int_{\mathcal{V}(t)} \nabla \mathbf{u}(\mathbf{u} - \frac{\partial d}{\partial t}) dx = \int_{J\hat{\mathcal{V}}} ((\nabla \mathbf{u}) F^{-1}(\mathbf{u} - \frac{\partial d}{\partial t}) dx \tag{3.10}$$

$$\int_{\mathcal{V}(t)} \nabla \cdot \mathbf{u} dx = \int_{\hat{\mathcal{V}}} \nabla \cdot (JF^{-1}\mathbf{u}) dx \tag{3.11}$$

$$\int_{\mathcal{V}(t)} \nabla \cdot \sigma_f dx = \int_{\hat{\mathcal{V}}} \nabla \cdot (JF^{-1}\hat{\sigma_f}) dx \tag{3.12}$$

$$\hat{\sigma_f} = -pI + \mu(\nabla \mathbf{u} F^{-1} + F^{-T}\mathbf{u}^T) \tag{3.13}$$

**Assembling all these terms together with** (2.2) **gives the fluid equations from a reference frame**:

$$\rho_f J\big(\frac{\partial \mathbf{u}}{\partial t} dx + (\nabla \mathbf{u}) F^{-1}(\mathbf{u} - \frac{\partial \mathbf{d}}{\partial t})\big) = \nabla \cdot (JF^{-1}\hat{\sigma_f}) + J\rho_f f \tag{3.14}$$

$$\nabla \cdot (JF^{-1}\mathbf{u}) = 0 \tag{3.15}$$

## 3.3 Lifting operators for upholding mesh quality

Using the ALE method the solid domain moves into to fluid domain. The deformations from the structure through the interface are extrapolated to the fluid domain using different lifting operators. The lifting operators redistributes the interior node locations to uphold the mesh quality. The choice of lifting operator is important for the overall FSI problem to be calculated [15]. When large deformations occur, we need a good lifting operator to uphold the integrity of the computing domain. A poor choice will make the mesh overlap and singularities may occur. When extrapolating deformation from the solid to the fluid domain, the fluid domain itself acts as a structure, deforming according to the deformations from the structure domain.

I will in this section present different lifting operators, that act differently on the computational domain. In **??** the techniques will be tested and investigated.

### 3.3.1 Harmonic extension

For small to moderate deformations an harmonic extension can be used. The harmonic extension uses the Laplace equation, transporting the deformations from the solid into the fluid domain. A variable $\alpha_u > 0$ can be multiplied to the Laplace equation, to control the amount of lifting of deformations to the fluid domain.

$$-\alpha_u \nabla^2 \mathbf{d} = 0 \quad in \ \hat{\mathcal{F}} \tag{3.16}$$

$$\mathbf{d} = 0 \quad on \ \partial\hat{\mathcal{F}}/\hat{\Sigma} \tag{3.17}$$

$$\mathbf{d}_f = \mathbf{d}_s \quad on \ \hat{\Sigma} \tag{3.18}$$

When using the harmonic lifting operator the variable $\alpha_u$ is very important when calculating moderate deformations. For small deformations a constant can be used for $\alpha_u$. But for larger deformations we need to be a bit more clever. A good strategy for choosing $\alpha_u$ is proposed by Wick in [15], and further discussed in [9] and [7]. This alpha gets bigger when closer to the interface:

$$\alpha_u = \frac{1}{x^q} \tag{3.19}$$

where $x^q$ is the distance from the interface. If $q = 0$ the laplacian i recovered. When the distance becomes larger, $\alpha_u$ gets smaller, and vice versa. Defining $\alpha_u$ in this manner is a smart choice since it upholds the cell structure closer to the interface where most of the cell distortion appears.

### 3.3.2 Biharmonic extension

The last extension is the biharmonic extension. The biharmonic extension provides more freedom than the harmonic and linear elastic in choosing boundary conditions and choice of parameter $\alpha_u > 0$. This is because the biharmonic extension, extends the deformation in a manner that upholds the integrity of the cells even in large deformations, even with $\alpha_u$ as a constant. In its simplest form it is written as:

$$-\alpha_u \nabla^4 \mathbf{d} = 0 \quad in \ \hat{\mathcal{F}} \tag{3.20}$$

The biharmonic extension is calculated with a mixed formulation where we introduce a new function $\omega$ (not to be confused with the domain velocity), the function is added to the system so that we solve for 4 functions:

$$\omega = \alpha_u \nabla^2 \mathbf{d} \quad and \quad -\alpha_u \nabla^2 \omega = 0 \ in \ \hat{\mathcal{F}} \tag{3.21}$$

with the two types of boundary conditions. The first boundary conditions being:

$$\mathbf{d} = \partial_n \mathbf{d} = 0 \quad on \ \partial\hat{\mathcal{F}} \setminus \hat{\Sigma} \tag{3.22}$$

$$\mathbf{d}_f = \mathbf{d}_s \quad on \ \hat{\Sigma} \tag{3.23}$$

The second type of boundary condition imposes conditions on $\mathbf{d}$ and $\omega$, and are written in terms of single component functions $d^{(1)}, d^{(2)}$ and $\omega^{(1)}, \omega^{(2)}$

$$\mathbf{d}^{(1)} = \partial_n \mathbf{d}^{(1)} = 0, and \quad \omega^{(1)} = \partial_n \omega^{(1)} = 0 \quad on \ \partial\hat{\mathcal{F}}_{in,out} \tag{3.24}$$

$$\mathbf{d}^{(2)} = \partial_n \mathbf{d}^{(2)} = 0, and \quad \omega^{(2)} = \partial_n \omega^{(2)} = 0 \quad on \ \partial\hat{\mathcal{F}}_{walls} \tag{3.25}$$

$$\tag{3.26}$$

Since the biharmonic extension is of fourth order character it will have a higher computational cost [8] than the harmonic or linear elastic.

## 3.4 Interface conditions

Figure 3.1 shows a typical Fluid Structure Interaction domain. The fluid is surrounded by elastic walls, like for instance a blood vessel. Inflow of fluid at $\partial\hat{\mathcal{F}}_{in}$, a change in pressure, or a motion of the solid determines the flow of the fluid. The fluid's stress on the walls causes deformation in the solid domain and vice versa. The interface is where these energies are transferred and we therefore need conditions on the interface.

The three interface conditions comes from simple physical properties and consist of [8]:

- *Kinematic condition*: $\mathbf{u}_f = \mathbf{u}_s \ on \ \hat{\Sigma}$. The fluid and structure velocities are equal on the interface. Meaning the fluid moves with the interface at all times.
  Since we use a global function for $\mathbf{u}$ in both fluid and structure domains,

this condition is upheld.
The fluid and solid velocities are usually in different coordinate systems, the solid velocity is then not available in Eulerian Coordinates. We instead link fluid velocity at the interface by using the fact that $\mathbf{u}_s = \frac{\partial \mathbf{d}}{\partial t}$. Setting $\mathbf{u}_f = \frac{\partial \mathbf{d}}{\partial t}$ at the interface.

- *Dynamic condition*: $\sigma_f n_f = \sigma_s n_s \ on \ \hat{\Sigma}$.
The dynamic interface condition relates to Newtons third law of action and reaction. The forces on the interface area, here written as the normal forces are balanced on the interface. These forces will be written in a Lagrangian formulation:
$J\sigma_f F^{-T} n_f = P n_s \ on \ \hat{\Sigma}$.
The dynamic condition is a Neumann condition that belongs to both subproblems.

- *Geometrical condition*: This condition says that the fluid and structure domains do not overlap, but rather that elements connect so the functions needing to transfer force are continuos across the entire domain.

## 3.5 Discretization of monolithic FSI equations

After introducing all the equations and boundary conditions needed to solve a FSI problem. We are ready to discretize the equations into one monolithic scheme. The equations will be discretized and solved using finite difference and finite element methods. I will introduce a so called $\theta$-scheme which will make it easy to implement different schemes, by choosing a value for $\theta$. I will briefly introduce the spaces needed to discretize, following the ideas and notations of [14]:

### Spaces

Let $X \in \mathbb{R}^d, d \in \{1, 2\}$ be a time dependent domain we define:

$$\hat{V}_X := H^1(X), \qquad \hat{V}_X^1 := H_0^1(X) \tag{3.27}$$

$H^1$ indicating a Hilbert space and

$$\hat{L}_X := L^2(X), \qquad \hat{L}_X^0 := L^2(X)/\mathbb{R} \tag{3.28}$$

$L^2$ indicating a standard Lebesque space.

The trial and test spaces for the velocity variable in the fluid domain are defined as:

$$\hat{V}^0_{f,u} := \{\hat{u} \in H^1_0(\mathcal{F}) : \hat{u}_f = \hat{u}_s \ on \ \hat{\Sigma}\} \tag{3.29}$$

The artificial displacement spaces in the moving fluid domain are defined:

$$\hat{V}^0_{f,d} := \{\hat{d} \in H^1_0(\mathcal{F}) : \hat{d}_f = \hat{d}_s \ on \ \hat{\Sigma}\} \tag{3.30}$$

$$\hat{V}^0_{f,d} := \{\hat{d} \in H^1_0(\mathcal{F}) : \hat{\psi}_f = \hat{\psi}_s \ on \ \hat{\Sigma}\} \tag{3.31}$$

**Discretization**

The temporal discretization is done using finite difference schemes and the spatial is treated with the finite element method. Employing a so called $\theta-$ scheme that will enables us to easily switch between schemes.

In the domain $\Omega$ and time interval [0,T]:

Find $U = \{\mathbf{u}, \mathbf{d}, p\} \in \hat{X}^0_D$ where $\hat{X}^0_D := \{\mathbf{u}^D_f + \hat{V}^0_{f,\mathbf{u}}\} \times \hat{L}_f \times \{\mathbf{d}^D_f + \hat{V}^0_{f,\hat{f}}\} \times \{\mathbf{d}^D_f + \hat{V}^0_{f,\hat{f}}\} \times \hat{L}^0_f \times \hat{L}^0_s$ such that:

$$\int_0^T A(U)(\Psi)dt = \int_0^T \hat{F}(\Psi)dt \quad \forall \Psi \in \hat{X} \tag{3.32}$$

where $\Psi = \{\phi, \psi, \gamma\}$

$\hat{X} = \hat{V}^0_{f,\mathbf{u}} \times \hat{L}_f \times \hat{V}^0_{f,\mathbf{d},\hat{\Sigma}} \times \hat{V}^0_s \times \hat{L}^0_f \times \hat{L}^0_s$

I first introduce the scheme using, for simplicity, the harmonic mesh motion. Let $\mathbf{u}$ be a global function in the entire domain instead of $\mathbf{u}_f$ in the fluid and $\mathbf{u}_s$ in the solid. Same for the test functions. This is done for ease of reading and also for the ease of implementation later.

**The full monolithic FSI variational form reads**:

$$
\begin{aligned}
A(U) = &(J\rho_f \partial_t \mathbf{u}, \phi) - (J(\nabla \mathbf{u})F^{-1}(\mathbf{u} - \partial_t d), \phi)_{\hat{\mathcal{F}}} && (3.33)\\
&+ (J\sigma_f F^{-T}, \nabla\phi)_{\hat{\mathcal{F}}} && (3.34)\\
&+ (\rho_s \partial_t \mathbf{u}, \phi)_{\hat{\mathcal{S}}} + \big(P, \nabla\phi\big)_{\hat{\mathcal{S}}} && (3.35)\\
&+ (\alpha_u \nabla \mathbf{u}, \nabla\psi)_{\hat{\mathcal{F}}} + (\nabla \cdot (JF^{-1}\mathbf{u}), \gamma)_{\hat{\mathcal{F}}} && (3.36)\\
&+ \delta\big((\partial_t \mathbf{d}, \psi)_{\hat{\mathcal{S}}} - (\mathbf{u}, \psi)_{\hat{\mathcal{S}}}\big) && (3.37)\\
&+ \big(J\sigma_{f,p}F^{-T}, \nabla\phi\big) && (3.38)
\end{aligned}
$$

The condition (3.37), is weighted with a $\delta$ value. This is a critical detail for the program (detailed later) to run. The weighting says in a weak manner that this condition is important for the overall program.

Introducing the *One step-$\theta$ scheme* from [14], which has the advantage of easily being changed from a backward (implicit), forward(explicit), or a Crank-Nicholson (implicit) scheme, by changing the value of $\theta$. The Crank-Nicholson scheme is of second order, but suffers from instabilities in this monolithic scheme for certain time step values [14]. A remedy for these instabilities is to chose a Crank-Nicholson scheme that is shifted towards the implicit side. How this is done will become evident once the scheme is defined.

The variational form is defined by dividing into four categories. This may seem strenuous at first, but the need for it will become evident when implementing the $\theta$-scheme. The four divided categories consists of: a time group $A_T$(with time derivatives), implicit $A_I$, pressure $A_P$ and the rest $A_E$ (stress terms and convection):

$$
\begin{aligned}
A_T(U) = &(J\rho_f \partial_t \mathbf{u}, \phi) - (J(\nabla \mathbf{u})F^{-1}(\partial_t \mathbf{d}), \phi)_{\hat{\mathcal{F}}} && (3.39)\\
&+ (\rho_s \partial_t \mathbf{u}, \phi)_{\hat{\mathcal{S}}} + (\partial_t \mathbf{d}, \psi)_{\hat{\mathcal{S}}} && (3.40)\\
A_I(U) = &(\alpha_u \nabla \mathbf{u}, \nabla\psi)_{\hat{\mathcal{F}}} + (\nabla \cdot (JF^{-1}\mathbf{u}), \gamma)_{\hat{\mathcal{F}}} && (3.41)\\
A_E(U) = &(J(\nabla u)F^{-1}\mathbf{u}, \phi)_{\hat{\mathcal{F}}} + (J\sigma_{f,u}F^{-T}, \nabla\phi)_{\hat{\mathcal{F}}} && (3.42)\\
&+ \big(P, \nabla\phi\big)_{\hat{\mathcal{S}}} - (\mathbf{u}, \psi)_{\hat{\mathcal{S}}} && (3.43)\\
A_P(U) = &\big(J\sigma_{f,p}F^{-T}, \nabla\phi\big) && (3.44)
\end{aligned}
$$

Notice that the fluid stress tensors have been split into a velocity and pressure

part.

$$\sigma_{f,u} = \mu(\nabla u F^{-1} + F^{-T}\nabla u) \tag{3.45}$$
$$\sigma_{f,p} = -pI \tag{3.46}$$

For the time group, discretization is done in the following way:

$$A_T(U^{n,k}) \approx \frac{1}{k}\big(\rho_f J^{n,\theta}(\mathbf{u}^n - \mathbf{u}^{n-1}), \phi\big)_{\hat{\mathcal{F}}} - \frac{1}{k}\big(\rho_f(\nabla u)(\mathbf{d}^n - \mathbf{d}^{n-1}), \phi\big)_{\hat{\mathcal{F}}} \tag{3.47}$$
$$+\frac{1}{k}\big(\rho_s(\mathbf{u}^n - \mathbf{u}^{n-1}), \phi\big)_{\hat{\mathcal{S}}} + \frac{1}{k}\big((\mathbf{d}^n - \mathbf{d}^{n-1}), \psi\big)_{\hat{\mathcal{S}}} \tag{3.48}$$

The Jacobian is written with superscript $\theta$ as:

$$J^{n,\theta} = \theta J^n + (1-\theta)J^{n-1} \tag{3.49}$$

Finally we can introduce the *One step-$\theta$ scheme*: Find $U^n = \{\mathbf{u}^n, \mathbf{d}^n, p^n\}$

$$A_T(U^{n,k}) + \theta A_E(U^n) + A_P(U^n) + A_I(U^n) = \tag{3.50}$$
$$-(1-\theta)A_E(U^{n-1}) + \theta\hat{f}^n + (1-\theta)\hat{f}^{n-1} \tag{3.51}$$

Notice that the scheme is selected by the choice of $\theta$. By choosing $\theta = 1$ we get the back Euler scheme, for $\theta = \frac{1}{2}$ we get the Crank-Nicholson scheme and for the shifted Crank-Nicholson we set $\theta = \frac{1}{2} + k$, effectively shifting the scheme towards the implicit side. $\hat{f}$ is the body forces. The shifting of the scheme towards the implicit side is important for long term stability for certain time step values [14]. The shifting will be investigated in chaper **??**.

# Appendices

# Appendix A

# Appendix

## A.1 Lagrangian physics

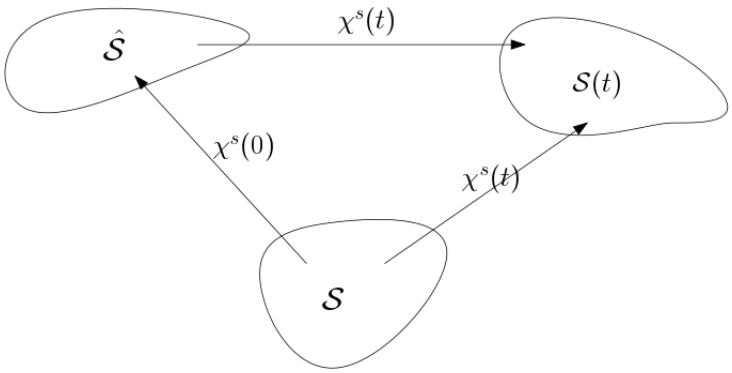


Let $\hat{\mathcal{S}}$, $\mathcal{S}$, $\mathcal{S}(t)$ be the initial stress free configuration of a given body, the reference and the current configuration respectively. I define a smooth mapping from the reference configuration to the current configuration:

$$\chi^s(\mathbf{X}, t) : \hat{\mathcal{S}} \to \mathcal{S}(t) \tag{A.1}$$

Where $\mathbf{X}$ denotes a material point in the reference domain and $\chi^s$ denotes the mapping from the reference configuration to the current configuration. Let $d^s(\mathbf{X}, t)$ denote the displacement field which describes deformation on a body. The mapping $\chi^s$ can then be specified from a current position plus the displacement from that position:

$$\chi^s(\mathbf{X}, t) = \mathbf{X} + d^s(\mathbf{X}, t) \tag{A.2}$$

which can be written in terms of the displacement field:

$$d^s(\mathbf{X}, t) = \chi^s(\mathbf{X}, t) - \mathbf{X} \tag{A.3}$$

Let w($\mathbf{X}$,t) be the domain velocity which is the partial time derivative of the displacement:

$$w(\mathbf{X}, t) = \frac{\partial \chi^s(\mathbf{X}, t)}{\partial t} \tag{A.4}$$

### A.1.1 Deformation gradient

The deformation gradient describes the rate at which a bode undergoes deformation. Let $d(\mathbf{X}, t)$ be a differentiable deformation field in a given body, the deformation gradient is then:

$$F = \frac{\partial \chi^s(\mathbf{X}, t)}{\partial \mathbf{X}} = \frac{\partial \mathbf{X} + d^s(\mathbf{X}, t)}{\partial \mathbf{X}} = I + \nabla d(\mathbf{X}, t) \tag{A.5}$$

which denotes relative change of position under deformation in a Lagrangian frame of reference. We can observe that when there is no deformation. The deformation gradient $F$ is simply the identity matrix.

Let the Jacobian determinant, which is the determinant of the of the deformation gradient F, be defined as:

$$J = \det(F) \tag{A.6}$$

The Jacobian determinant is used to change between volumes, assuming infinitesimal line and area elements in the current $ds, dx$ and reference $dV, dX$ configurations. The Jacobian determinant is therefore known as a volume ratio.

### A.1.2 Strain

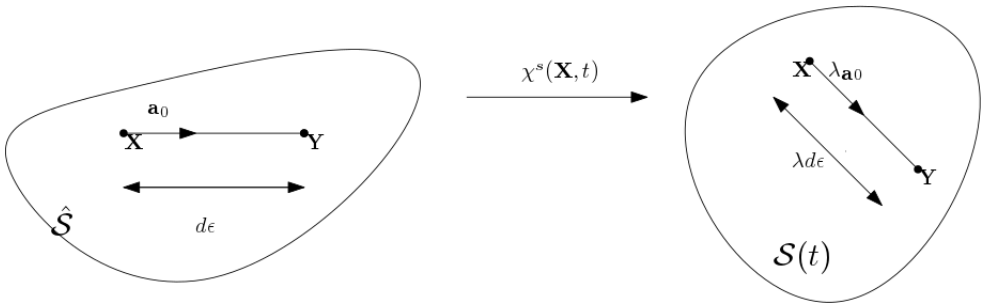


Figure A.1: Deformation of a line element with length $d\epsilon$ into a line element with length $\lambda d\epsilon$

Strain is the relative change of location between two particles. Strain, strain rate and deformation is used to describe the relative motion of particles in a continuum. This is the fundamental quality that causes stress [8].

Observing two neighboring points $\mathbf{X}$ and $\mathbf{Y}$. Let $\mathbf{Y}$ be described by adding and subtracting the point $\mathbf{X}$ and rewriting $\mathbf{Y}$ from the point $\mathbf{X}$ plus a distance $d\mathbf{X}$ :

$$\mathbf{Y} = \mathbf{Y} + \mathbf{X} - \mathbf{X} = \mathbf{X} + |\mathbf{Y} - \mathbf{X}|\frac{\mathbf{Y} - \mathbf{X}}{|\mathbf{Y} - \mathbf{X}|} = \mathbf{X} + d\mathbf{X} \tag{A.7}$$

Let $d\mathbf{X}$ be denoted by:

$$d\mathbf{X} = d\epsilon\mathbf{a}_0 \tag{A.8}$$
$$d\epsilon = |\mathbf{Y} - \mathbf{X}| \tag{A.9}$$
$$\mathbf{a}_0 = \frac{\mathbf{Y} - \mathbf{X}}{|\mathbf{Y} - \mathbf{X}|} \tag{A.10}$$

where $d\epsilon$ is the distance between the two points and $\mathbf{a}_0$ is a unit vector

We see now that $d\mathbf{X}$ is the distance between the two points times the unit vector or direction from $\mathbf{X}$ to $\mathbf{Y}$.

A certain motion transform the points $\mathbf{Y}$ and $\mathbf{X}$ into the displaced positions $\mathbf{x} = \chi^s(\mathbf{X}, t)$ and $\mathbf{y} = \chi^s(\mathbf{Y}, t)$. Using Taylor?s expansion $\mathbf{y}$ can be expressed in terms of the deformation gradient:

$$\mathbf{y} = \chi^s(\mathbf{Y}, t) = \chi^s(\mathbf{X} + d\epsilon\mathbf{a}_0, t) \tag{A.11}$$
$$= \chi^s(\mathbf{X}, t) + d\epsilon F\mathbf{a}_0 + \mathcal{O}(\mathbf{Y} - \mathbf{X}) \tag{A.12}$$

where $\mathcal{O}(\mathbf{Y} - \mathbf{X})$ refers to the small error that tends to zero faster than $(\mathbf{X} - \mathbf{Y}) \to \mathcal{O}$.

Setting $\mathbf{x} = \chi^s(\mathbf{X}, t)$ It follows that:

$$\mathbf{y} - \mathbf{x} = d\epsilon F\mathbf{a}_0 + \mathcal{O}(\mathbf{Y} - \mathbf{X}) \tag{A.13}$$
$$= F(\mathbf{Y} - \mathbf{X}) + \mathcal{O}(\mathbf{Y} - \mathbf{X}) \tag{A.14}$$

Let the **stretch vector** be $\lambda_{\mathbf{a}0}$, which goes in the direction of $\mathbf{a}_0$:

$$\lambda_{\mathbf{a}0}(\mathbf{X}, t) = F(\mathbf{X}, t)\mathbf{a}_0 \tag{A.15}$$

Looking at the square of $\lambda$:

$$\lambda^2 = \lambda_{\mathbf{a}0}\lambda_{\mathbf{a}0} = F(\mathbf{X}, t)\mathbf{a}_0 F(\mathbf{X}, t)\mathbf{a}_0 \tag{A.16}$$
$$= \mathbf{a}_0 F^T F\mathbf{a}_0 = \mathbf{a}_0 C\mathbf{a}_0 \tag{A.17}$$

We have not introduced the important right Cauchy-Green tensor:

$$C = F^T F \tag{A.18}$$

Since $\mathbf{a}_0$ is just a unit vector, we see that C measures the squared length of change under deformation. We see that in order to determine the stretch one needs only the direction of $\mathbf{a}_0$ and the tensor C. C is also symmetric and positive definite $C = C^T$. I also introduce the Green-Lagrangian strain tensor E:

$$E = \frac{1}{2}(F^T F - I) \tag{A.19}$$

which is also symmetric since C and I are symmetric. The Green-Lagrangian strain tensor E has the advantage of having no contributions when there is no deformations. Where the Cauchy-Green tensor gives the identity matrix for zero deformation.

### A.1.3 Stress

While strain, deformation and strain rate only describe the relative motion of particles in a given volume, stress give us the internal forces between neighboring particles. Stress is responsible for deformation and is therefore crucial in continuum mechanics. The unit of stress is force per area.

that completely define the state of stress at a point inside a material in the deformed state, placement, or configuration. The tensor relates a unit-length direction vector n to the stress vector T(n) across an imaginary surface perpendicular to n:

Introducing the Cauchy stress tensor $\sigma_s$, which define the state of stress inside a material. The version of Cauchy stress tensor is defined by the material model used. If we use this tensor on an area, taking the stress tensor times the normal vector $\sigma_s \mathbf{n}$ we get the forces acting on that area.

Stress tensor defined from the Cauchy by the constitutive law of St. Venant-Kirchhoff hyperelastic material model:

$$\sigma_s = \frac{1}{J} F(\lambda_s(trE)I + 2\mu_s E)F^T \tag{A.20}$$

Using the deformation gradient and the Jacobian determinant., I get the first Piola-Kirchhoff stress tensor P:

$$P = J\sigma F^{-T} \tag{A.21}$$

This is known as the *Piola Transformation* and maps the tensor into a Lagrangian formulation which will be used when stating the solid equation.

Introducing the second Piola-Kirchhoff stress tensor S:

$$S = JF^{-1}\sigma F^{-T} = F^{-1}P = S^T \tag{A.22}$$

from this relation the first Piola-Kirchhoff tensor can be expressed by the second:

$$P = FS \tag{A.23}$$

## A.2 Results

**Table 3** Results for unsteady benchmark FSI3.

| | Unknowns | $\Delta t$ | $u_1(A)$ [$\times 10^{-3}$] | $u_2(A)$ [$\times 10^{-3}$] | $F_D$ | $F_L$ |
|---|---|---|---|---|---|---|
| 1 | 61318 | 1.0e−3 | −2.54 ± 2.41 | 1.45 ± 32.80 | 450.3 ± 23.51 | -0.10 ± 143.0 |
| | 237286 | 2.0e−3 | −2.88 ± 2.73 | 1.53 ± 34.94 | 458.6 ± 27.18 | 2.08 ± 153.1 |
| | 237286 | 1.0e−3 | −2.87 ± 2.73 | 1.54 ± 34.94 | 458.6 ± 27.31 | 2.00 ± 153.3 |
| | 237286 | 5.0e−4 | −2.86 ± 2.72 | 1.53 ± 34.90 | 458.6 ± 27.27 | 2.01 ± 153.4 |
| | 941158 | 1.0e−3 | −2.91 ± 2.77 | 1.47 ± 35.26 | 459.9 ± 27.92 | 1.84 ± 157.7 |
| 2a | 11250 | 5.0e−3 | −2.48 ± 2.24 | 1.27 ± 36.50 | – | – |
| 2b | 7176 | 5.0e−3 | −2.44 ± 2.32 | 1.02 ± 31.82 | 473.5 ± 56.97 | 8.08 ± 283.8 |
| | 7176 | 2.0e−3 | −2.48 ± 2.39 | 0.92 ± 32.81 | 471.3 ± 62.28 | 6.11 ± 298.6 |
| | 7176 | 1.0e−3 | −2.58 ± 2.49 | 0.94 ± 33.19 | 470.4 ± 64.02 | 4.65 ± 300.3 |
| | 27744 | 5.0e−3 | −2.43 ± 2.27 | 1.41 ± 31.73 | 483.7 ± 22.31 | 2.21 ± 149.0 |
| | 27744 | 2.0e−3 | −2.63 ± 2.61 | 1.46 ± 33.46 | 483.3 ± 24.48 | 2.08 ± 161.2 |
| | 27744 | 1.0e−3 | −2.80 ± 2.64 | 1.45 ± 34.12 | 483.0 ± 25.67 | 2.21 ± 165.3 |
| | 42024 | 2.5e−3 | −2.40 ± 2.26 | 1.39 ± 31.71 | 448.7 ± 21.16 | 1.84 ± 141.3 |
| | 42024 | 1.0e−3 | −2.53 ± 2.38 | 1.40 ± 32.49 | 449.7 ± 22.24 | 1.61 ± 142.8 |
| | 42024 | 5.0e−4 | −2.57 ± 2.42 | 1.42 ± 32.81 | 450.1 ± 22.49 | 1.49 ± 143.7 |
| | 72696 | 2.5e−3 | −2.64 ± 2.48 | 1.38 ± 33.25 | 451.1 ± 24.57 | 2.04 ± 150.6 |
| | 72696 | 1.0e−3 | −2.79 ± 2.62 | 1.28 ± 34.61 | 452.0 ± 25.78 | 1.91 ± 152.7 |
| | 72696 | 5.0e−4 | −2.84 ± 2.67 | 1.28 ± 34.61 | 452.4 ± 26.19 | 2.36 ± 152.7 |
| 3 | 19488 | 1.0e−3 | −3.02 ± 2.83 | 1.41 ± 35.47 | 458.2 ± 28.32 | 2.41 ± 145.6 |
| | 19488 | 5.0e−4 | −3.02 ± 2.85 | 1.42 ± 35.63 | 458.7 ± 28.78 | 2.23 ± 146.0 |
| | 19488 | 2.5e−4 | −3.02 ± 2.85 | 1.32 ± 35.73 | 458.7 ± 28.80 | 2.23 ± 146.0 |
| | 76672 | 1.0e−3 | −2.78 ± 2.62 | 1.44 ± 34.36 | 459.1 ± 26.63 | 2.41 ± 151.3 |
| | 76672 | 5.0e−4 | −2.78 ± 2.62 | 1.44 ± 34.35 | 459.1 ± 26.62 | 2.39 ± 150.7 |
| | 76672 | 2.5e−4 | −2.77 ± 2.61 | 1.43 ± 34.43 | 459.1 ± 26.50 | 2.36 ± 149.9 |
| | 304128 | 1.0e−3 | −2.86 ± 2.70 | 1.45 ± 34.93 | 460.2 ± 27.65 | 2.47 ± 154.9 |
| | 304128 | 5.0e−4 | −2.86 ± 2.70 | 1.45 ± 34.90 | 460.2 ± 27.47 | 2.37 ± 153.8 |
| | 304128 | 2.5e−4 | −2.88 ± 2.72 | 1.47 ± 34.99 | 460.5 ± 27.74 | 2.50 ± 153.9 |
| 4 | 81120 | 9.0e−5 | −5.18 ± 5.04 | 1.12 ± 45.10 | 477.0 ± 48.00 | 7.00 ± 223.0 |
| | 324480 | 2.0e−5 | −4.54 ± 4.34 | 1.50 ± 42.50 | 467.5 ± 39.50 | 16.20 ± 188.7 |
| 5 | 2480814 | 5.1e−5 | −2.88 ± 2.71 | 1.48 ± 35.10 | 463.0 ± 31.30 | 1.81 ± 154.0 |
| 6 | 7059 | 5.0e−4 | −1.60 ± 1.60 | 1.50 ± 25.90 | 525.0 ± 22.50 | -0.55 ± 106.0 |
| | 27147 | 5.0e−4 | −2.00 ± 1.89 | 1.45 ± 29.00 | 434.0 ± 17.50 | 2.53 ± 88.6 |
| 7 | 271740 | 5.0e−4 | −3.04 ± 2.87 | 1.55 ± 36.63 | 474.9 ± 28.12 | 3.86 ± 165.9 |

Figure A.2: Results from different contributions in from the paper Turek et.al 2010 [10]

[10]

# Bibliography


[1] K. Yusuf Billah. Resonance, Tacoma Narrows bridge failure, and undergraduate physics textbooks. *American Journal of Physics*, 59(2):118, 1991.

[2] David J Charlesworth. Solution of the Incompressible Navier- Stokes Equations on Unstructured Meshes by. (August), 2003.

[3] Charles L. Fefferman. Existence and smoothness of the Navier-Stokes equation. *The millennium prize problems*, (1):1–5, 2000.

[4] Miguel A. Fernández, Jimmy Mullaert, and Marina Vidrascu. Explicit robin-neumann schemes for the coupling of incompressible fluids with thin-walled structures. *Computer Methods in Applied Mechanics and Engineering*, 267:566–593, 2013.

[5] Miguel A. Fernández, Jimmy Mullaert, and Marina Vidrascu. Generalized Robin-Neumann explicit coupling schemes for incompressible fluid-structure interaction: Stability analysis and numerics. *International Journal for Numerical Methods in Engineering*, 101(3):199–229, 2015.

[6] Jie Liu, Rajeev K. Jaiman, and Pardha S. Gurugubelli. A stable second-order scheme for fluid-structure interaction with strong added-mass effects. *Journal of Computational Physics*, 270:687–710, 2014.

[7] Selim MM and Koomullil RP. Mesh Deformation Approaches – A Survey. *Journal of Physical Mathematics*, 7(2), 2016.

[8] Thomas Richter. Fluid Structure Interactions. 2016.

[9] K. Stein, T. Tezduyar, and R. Benney. Mesh Moving Techniques for Fluid-Structure Interactions With Large Displacements. *Journal of Applied Mechanics*, 70(1):58, 2003.

[10] S Turek, J Hron, M Razzaq, H Wobker, and M Sch. Fluid Structure Interaction II. 73, 2010.

[11] Boris Valkov, Chris H Rycroft, and Ken Kamrin. Eulerian method for fluid – structure interaction and submerged solid – solid contact problems.

[12] E. H. van Brummelen. Added Mass Effects of Compressible and Incompressible Flows in Fluid-Structure Interaction. *Journal of Applied Mechanics*, 76(2):021206, 2009.

[13] Frank M White. Viscous Fluid Flow Viscous. *New York*, Second:413, 2000.

[14] Thomas Wick. Adaptive Finite Element Simulation of Fluid-Structure Interaction with Application to Heart-Valve Dynamics. *Institute of Applied Mathematics, University of Heidelber*, page 157, 2011.

[15] Thomas Wick. Fluid-structure interactions using different mesh motion techniques. *Computers and Structures*, 89(13-14):1456–1467, 2011.